

Original Article

Cite this article: Kühn D, Hainzl S, Dahm T, Richter G, and Vera Rodriguez I. A review of source models to further the understanding of the seismicity of the Groningen field.

Netherlands Journal of Geosciences, Volume 101, e11. <https://doi.org/10.1017/njg.2022.7>

Received: 29 November 2021

Revised: 9 March 2022


Accepted: 7 April 2022

Keywords:

deterministic; empirical; hybrid; machine learning; seismicity model

Author for correspondence: Daniela Kühn,
Email: daniela@norsar.no

A review of source models to further the understanding of the seismicity of the Groningen field

Daniela Kühn^{1,2} , Sebastian Hainzl², Torsten Dahm^{2,3}, Gudrun Richter² and Ismael Vera Rodriguez¹

¹NORSAR, Kjeller, Norway; ²GFZ German Research Centre for Geosciences, Potsdam, Germany and ³University of Potsdam, Potsdam, Germany

Abstract

The occurrence of felt earthquakes due to gas production in Groningen has initiated numerous studies and model attempts to understand and quantify induced seismicity in this region. The whole bandwidth of available models spans the range from fully deterministic models to purely empirical and stochastic models. In this article, we summarise the most important model approaches, describing their main achievements and limitations. In addition, we discuss remaining open questions and potential future directions of development.

Introduction

Seismicity models form the backbone of probabilistic seismic hazard assessment (PSHA) for tectonic and induced earthquakes. They describe the frequency-magnitude distribution and the earthquake rate in space and time. Except for the occurrence of aftershock sequences, tectonic seismicity can be well described by a stationary process, and because of this, empirical fits of the declustered, observed seismicity data can be used to forecast future activity. In contrast, anthropogenic seismicity is time-dependent because it is related to activities such as, for instance, gas production. Forecasting and modelling the expected time dependence of future seismic activity requires an understanding of the physical processes involved in earthquake nucleation.

Stress changes are believed to be the main cause of seismicity. In particular, the Coulomb failure stress (CFS) is a key parameter controlling rock failure and earthquake nucleation (Okada, 1992; King et al., 1994). The reasons for stress changes can be manifold, such as earthquake-induced or poroelastic changes due to fluid injection or extraction (e.g., Geertsma, 1973; Segall, 1989). Besides estimating the expected stress changes, models need to define the corresponding seismicity response function. For this purpose, physical models use constitutive friction relations. While simple static-kinetic friction relationships predict an immediate response after a stress change, more complex relationships such as the rate- and state-dependent friction law (Ruina, 1983) explain delayed responses in seismicity.

Deterministic physical models based on CFS and friction laws can simulate earthquake nucleation, rupture propagation and stress changes on pre-defined neighbouring faults (Fig. 1a). They allow to address specific problems of earthquake patterns and to confirm or dismiss hypotheses, for example, to analyse the conditions for a rupture front propagating into the over- or underburden of the reservoir, which is important to estimate the maximum possible magnitude of triggered earthquakes. Their strength at the same time constitutes their Achilles' heel since models are highly specific, that is, adapted to individual scenarios. Thus, unknown initial conditions, structural settings, or material properties require running a large number of alternative scenarios to account for epistemic uncertainties and provide realistic forecasts. Due to the high computational costs of deterministic rupture simulations, their direct use for PSHA is very expensive.

On the other hand, more efficient, purely data-driven statistical models cannot easily account for transient driving forces (Fig. 1b). Two representatives of such models are the temporally stationary, spatially inhomogeneous Poisson model and the Epidemic-Type Aftershock Sequences (ETAS) model (Ogata, 1988, 1998). The ETAS model supplements the Poisson model with aftershock activity described by empirical relationships for aftershock productivity, Omori-type rate decay and distance decay. The standard ETAS model explains the short-term clustering of earthquakes but is unable to account for changing boundary conditions that lead to transient seismicity. Similar challenges apply to machine learning (ML), a third class of data-driven models (Jordan & Mitchell, 2015). Unlike physical modelling approaches, ML approaches learn directly from data without explicitly reasoning about the underlying physical mechanisms (Bergen et al., 2019) and thus avoid model biases due to incomplete process understanding.

© The Author(s), 2022. Published by Cambridge University Press on behalf of the Netherlands Journal of Geosciences Foundation. This is an Open Access article, distributed under the terms of the Creative Commons Attribution licence (<http://creativecommons.org/licenses/by/4.0/>), which permits unrestricted re-use, distribution and reproduction, provided the original article is properly cited.

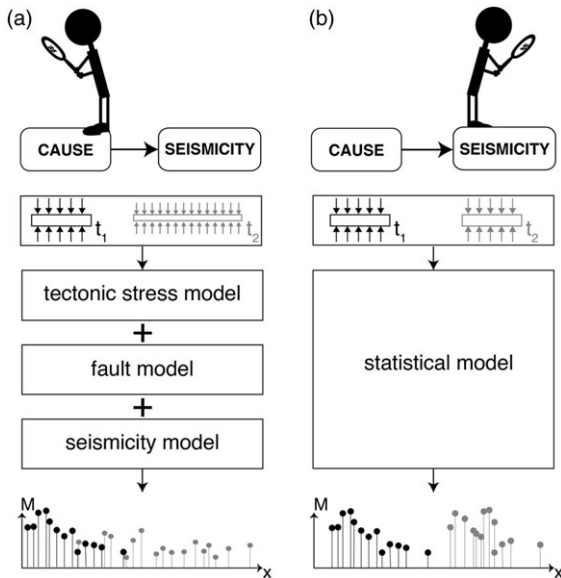


Fig. 1. Sketch of two end-member model types: (a) physical model comprising potentially highly specific model parts that can easily be adapted to model hitherto non-existing conditions (e.g., grey coloured seismicity related to future loading scenario at time t_2); and (b) generalised statistical model, simpler to apply, but limited to the conditions of the training datasets (e.g., forecasts at time t_2 only based on previous observations).

However, ML should not be used to extrapolate behaviour outside the parameter range of the training dataset. Thus, its accuracy and forecasting power are limited in the case of small training datasets, specifically if they are derived from transient processes.

While the empirical data-driven models ignore important physical knowledge and constraints, the model class of hybrid models combines the understanding of physical processes and statistical components and is thus most promising for seismic hazard assessment of anthropogenic seismicity. We will provide an overview on seismicity models applied to the Groningen field in the following, while more details, including a careful assessment of the advantages and disadvantages, can be found in Dahm *et al.* (2020b).

The occurrence of felt earthquakes accompanying gas production in Groningen, the Netherlands, is of high social importance and has initiated dense instrumentation and numerous field studies. Many of the more recent models for explaining and quantifying induced or triggered seismicity in the world have benefited from the outstanding comprehensive datasets collected at Groningen. This paper discusses the main categories of seismicity models at Groningen and potential future directions.

Seismicity models applied to the Groningen field

The Groningen gas reservoir and its seismicity already was the topic of numerous publications. For example, De Jager & Visser (2017) give an overview on its geology, Visser & Solano Viota (2017) and Van Oeveren *et al.* (2017) on the static and dynamic reservoir model, respectively, Van Thienen-Visser & Fokker (2017) on compaction and subsidence, Dost *et al.* (2017) on the development of seismicity, monitoring network and PSHA, Kortekaas & Jaarsma (2017) on the generation of an improved fault model, Bommer *et al.* (2017) on the development of a ground motion model, Kruiver *et al.* (2017) of a shear wave and

Hofman *et al.* (2017) of a shallow velocity model. The Groningen field, measuring approximately 30×30 km (Spiers *et al.*, 2017) and thus being one of the largest in the world, is located in the north-east of the Netherlands at a depth of approximately 3000 m. It consists of Slochteren sandstone sealed on the top by the Zechstein salt formation and is primarily limited in its lateral extents by fault closures. The net reservoir thickness increases from about 0 m to 280 m in a south-east to north-west direction (Bourne *et al.*, 2014), with seismic profiles showing the existence of numerous normal faults with variable spatial density mainly striking in NNW–SSE direction with secondary fault trends running E–W and N–S (De Jager & Visser, 2017) mostly dipping around 70° (Van Wees *et al.*, 2018). The presence of gas in Groningen was discovered in 1959, with production starting in 1963. The first seismic event related to gas extraction in Groningen was detected in 1991 (Van Eck *et al.*, 2006). Since then, more than 350 earthquakes with magnitude $M_L \geq 1.5$ have been recorded. Today, with more than 100 seismic stations operated by KNMI at an interstation distance smaller than 5 km, the Groningen area is one of the most thoroughly instrumented sites globally for monitoring of induced seismicity.

Over the monitoring period 1 April 1995 to 30 October 2012, it was assessed that less than 0.1% of the induced strain in Groningen had been accommodated by earthquakes; either aseismic deformation such as fault creep and ductile flow is dominant or induced strain is elastic and remains available to be released by future earthquakes (Bourne *et al.*, 2014). Especially in case of a termination of gas production in the near future, understanding the stress-induced seismicity is a challenge for seismicity models, since such a future stress scenario is not covered by the previous usage history.

Deterministic physical models

Several physical models were applied to model the seismicity of the Groningen field. Most researchers simplified the geometry to 2-D including only a single fault to investigate earthquake generation and rupture processes, but a 3-D model was developed as well to investigate the total fault slip (Sanz *et al.*, 2015).

Van Wees *et al.* (2014, 2017) studied the quasi-static nucleation and rupture of earthquakes on a fault offsetting a reservoir. Model dimensions of $6 \times 6 \times 6$ km were considered to be representative for major fault zones in the central area of the Groningen field. The model explains why earthquakes occur at pre-existing faults, since CFSs are far more pronounced on faults bounding or offsetting the reservoir than elsewhere. Assuming not critically stressed faults at the onset of the depletion, the model further explains the delayed onset of induced seismicity and the non-linear release of seismic moment observed in Groningen (Bourne *et al.*, 2014). However, the overall characteristics (a Gutenberg–Richter b -value of approximately one and a maximum observed magnitude of $M_{\max} \approx 3.6$) can only be reproduced if the fault is critically stressed from the beginning. These limitations may result from considering only a single fault, whereas many faults with different orientations are present in the Groningen field. In addition, Van Wees *et al.* (2014, 2017) neglect the impact of absorption of stress by the salt cap rock and energy losses through aseismic slip, which may explain the overestimation of the seismic moment release.

For the same model set-up, Van den Bogert (2018) and Buijze *et al.* (2017, 2019) explored a fully dynamic initiation and propagation of ruptures in order to understand the impact of reservoir depletion, offset and thickness on the occurrence of fault instability

and earthquake magnitudes. The simulations showed that aseismic slip always precedes seismic ruptures in the nucleation phase, which accelerates to seismic slip when its size exceeds a critical length, thus corroborating the analytical expression derived by Uenishi & Rice (2003). The pressure drop necessary to initiate seismic ruptures was found to be independent of the reservoir width, but dependent on the slip-weakening relationship and the reservoir offset. Whereas larger fault offsets promote the nucleation of ruptures, they reduce the down-dip rupture size because ruptures were more easily arrested in stable stress regions. Propagation outside the reservoir interval is promoted by critical in situ stress, a large stress drop and small fracture energy (Buijze et al., 2019). Apart from the offset, the onset of fault slip is influenced by the orientation of the fault relative to the background stress field and the initial friction coefficient.

Zbinden et al. (2017) addressed the role of fluid flow in faults offsetting a reservoir similarly to Groningen. They used a fully coupled fluid flow and geomechanics 2-D simulator and found that stress-dependent permeability and linear poroelasticity played a major role in pore pressure and stress evolution within the fault. Especially, the fault strength was significantly reduced due to flow from the neighbouring reservoir compartment and other formations into the fault zone. In the case of well shut-in, a highly stressed fault zone could still be reactivated several decades after the production had ceased, although the shut-in resulted in a reduction of seismicity in general.

So far, 3-D reservoir models are restricted to quasi-static approaches, since stresses on faults offsetting the reservoir cannot be calculated by analytical expressions, particularly during rupture nucleation and propagation. Models of sufficient resolution to study the dynamic effects of seismic events are simply not feasible due to computational costs. An example of a 3-D fault model applied to the Groningen field is the finite-element model of Sanz et al. (2015), which consists of two detailed submodels with faults being embedded in a regional model. Such models can predict the cumulative fault slip but do not account for the nucleation and propagation of individual events. Thus, they can predict neither the radiated seismic energy and earthquake magnitude nor the relation between seismic and aseismic slip.

Since the Groningen field has long been produced with fluctuations in production rate over a range of timescales, DeDontney & Lele (2018) studied the impact of production fluctuations on seismicity and seismic hazard. First, they investigated the distance range influenced by daily and seasonal production variations using an analytic reservoir pressure model. Employing a rate-and-state (RS) model, they subsequently compared the seismicity rates for fluctuating and steady production schemes. In a third approach, the impact of such production schemes on seismic hazard was examined using an earthquake cycle model. The first model showed small pore pressure variations (approximately 0.1 bar) in the vicinity of wellbores (up to 200 m); since most faults are sufficiently far from wells, they should thus not be influenced by local production rates. The RS simulations demonstrated that clear seasonal seismicity rate changes are expected for the same stressing histories, but that high seismicity rates are required to conclusively reflect the signature of the imposed sinusoidal variation in stressing rate. In the third model, seismicity rates varied for fluctuating production rates and different parameters as well, but no change in the aggregate character of the seismicity and therefore, seismic hazard, was detected due to constant versus fluctuating production, since neither the cumulative number of events nor their magnitudes significantly changed over the year. However, the

choice of only a few fault dip and strike angles is not representative of the highly heterogeneous fault system and fault interactions in the Groningen field. The question if the catalogue of observed earthquakes exhibits a seasonality is still debated (Nepveu et al., 2016; Bierman et al., 2018; DeDontney & Lele, 2018; Park et al., 2018; Park & Nevenzeel, 2018).

As mentioned above, stresses on faults offsetting the reservoir could not be calculated by analytical expressions, restricting 3-D reservoir models to quasi-static approaches. However, Jansen et al. (2019) recently provided analytic expressions for a normal fault offsetting a homogeneous reservoir of infinite extension, which may enable computationally feasible 3-D dynamic fault simulations in the future.

Data-driven models

In contrast to the deterministic models, data-driven models estimate the relation between input (e.g., production rates) and output (seismicity) by data fitting, either by statistical approaches fitting parametric functions or ML approaches. The advantage of fully data-driven approaches is that the functional relationship between seismicity and driving mechanisms is not predetermined. Thus, data-driven models avoid any bias related to an incomplete understanding of the earthquake nucleation mechanism.

Statistical approaches

For the Groningen field, statistical model approaches differ in input data. Whereas DeDontney (2017) tested functional relations between local compaction of the reservoir and cumulative number of induced earthquakes, Hettema et al. (2017) and Vlek (2019) showed that the cumulative number of induced earthquakes accelerates as function of the cumulative volume extracted. Based on the fault slip model of Lele et al. (2016), DeDontney (2017) tested the same set of relationships between seismicity rate and fault slip instead of compaction. In areas in which a fault slip model exists, the fault slip-based metric yielded a significantly better representation of the observed seismicity than the compaction-based models. However, the model yielded the best results when a threshold in time was used to suppress modelled earthquakes at the beginning of gas production, indicating a physical inconsistency of the statistical model. In addition, although various functional forms fit the observed seismicity almost equally well, they resulted in very different activity forecasts over the next 10 years. This highlights the large epistemic uncertainty of predictions based on empirical functions and the insufficient size of the observed dataset.

A similar criticism can be expressed for the application of the ETAS model to Groningen seismicity. Since the ETAS model depends non-linearly on its model parameters, its forecasts are highly sensitive to the parameters estimated from the data. Thus, the input catalogue needs to include a sufficient number of aftershocks. The percentage of activity classified as aftershocks differs from ~5% (Muntendam-Bos, 2020) to 10–20% (Bourne et al., 2018) and 18–36% (Post et al., 2021), but likely does not fulfil this requirement.

For the model presented by Hettema et al. (2017) and Vlek (2019), it is noteworthy that if the Groningen reservoir is completely exploited, this model predicts a fixed number of future events independently of the production scenario. Consequently, lowering the annual production only postpones earthquakes. This behaviour results from the simple empirical relationship between the cumulative earthquake number and the cumulative

extracted gas volume, which has the advantage that time is eliminated as a variable, and short-term fluctuations on the order of months are suppressed. In combination with the empirical Gutenberg–Richter frequency–magnitude relation, the occurrence probabilities can be easily estimated for any magnitude range, in particular, the maximum expected magnitude (Vlek, 2019; Zöller & Holschneider, 2016). Nonetheless, the approach was only tested for the entire field without spatial resolution. The first test on different sub-regions of the Groningen field indicated that the empirical relation is not uniform and varies significantly in space, limiting the model's applicability (Hettema *et al.*, 2017).

ML approaches

Limbeck *et al.* (2018) and Lanz *et al.* (2019) applied ML to forecast production-induced seismicity in the Groningen field. While the model of Limbeck *et al.* (2018) was limited to a cumulative prediction of the earthquake numbers, Lanz *et al.* (2019) extended the model to predictions in time and space. The ML model was trained only with data recorded before the year 2013. The hold-out data between 2013 and 2016 were used to test the forecast power compared to two baseline models. The first assumed that the forecast rate was proportional to the change in depletion thickness, that is, pressure multiplied by reservoir thickness, while the other considered a proportionality to the change in strain thickness, that is, vertical strain multiplied by reservoir thickness.

The results of Lanz *et al.* (2019) demonstrated that ML models are able to qualitatively capture the decreasing trend in seismicity observed during the 2013–2016 hold-out period. However, although there was a relative match in trends, the models systematically underestimated seismicity. The random forest algorithm (Hastie *et al.*, 2009) yielded the best performance and a significantly better result than the two baseline models. In addition, the support vector machine with kernel function (Hastie *et al.*, 2009) showed significant improvements. The most significant spatial features were the topographic gradient of the reservoir, reservoir thickness variations along major faults and compressibility. Overall, however, static features had less impact than dynamic features such as pore pressure.

In any case, if the pressure development in the long term does not fall within the pressure range used in the training dataset, the ML model will likely lead to erroneous forecasts. In addition, important features are based on the results of the static and dynamic reservoir models, which in turn rest upon reservoir flow history matches and forecasts. Thus, the quality of the ML model depends on the quality of these input data. Confidence bands for the forecasts cannot be easily derived for the space-time ML model, and a separate magnitude model is required to complement the current spatiotemporal model.

Hybrid models

Most of the seismicity models applied to the Groningen field fall into the category of hybrid models. Due to their nature of combining physical models with statistical components, hybrid models differ notably in their level of sophistication.

One of the simplest approaches is the seismogenic index (SI) model (Shapiro *et al.*, 2010; Langenbruch & Zoback, 2016; Broccardo *et al.*, 2017). Although initially developed for fluid injections, it has been applied to fluid production as well (Shapiro, 2018). The SI model assumes that the earthquake rate is proportional to the flow rate, where the proportionality factor quantifies a seismogenic reaction of rocks to a unit volume fluid change. This

factor is estimated by empirical fits of fluid volumes to seismicity rates. The assumption that the ratio between earthquake number and fluid volume is constant relies on physical considerations. The model is based on the Gutenberg–Richter distribution and the application of an inhomogeneous Poisson model. The index is temporally invariable, since it represents a characteristic of the seismogenic state of a crustal volume independent of the anthropogenic perturbation. Shapiro (2018) estimated that in the Groningen field, the dominantly normal faulting conditions are unfavourable for seismicity induced by injection but favourable for earthquakes induced by production. Although the model has been demonstrated to work well for many injection sites, the assumed constant ratio between number of earthquakes and fluid volume contradicts the observed ratio increase with cumulative production volume in Groningen. In addition, the hydraulic diffusivity is expected to change over time due to compaction (Hettema *et al.*, 2017). So far, the model has not been demonstrated to fit the (spatio-)temporal distribution of seismicity in Groningen.

Wentinck (2015) postulated that during interseismic periods, the increase of shear stress on faults is proportional to the pressure drop. In contrast, earthquakes are assumed to lead to shear stress drops on faults proportional to the seismic moments of events. The likelihood of earthquake occurrences is described in his model by a Weibull probability distribution function. The model was applied to six relatively small regions (circular areas with a radius of ~5 km) within the Groningen, Annerveen and Eleveld fields. Overall, the model fitted the observed data well for each region, but so far was only tested assuming uniform pore pressure changes with a constant rate, which is an oversimplification. Thus, it is unclear whether more realistic spatiotemporal pressure data, despite continuing using uniform stress state model parameters, would lead to a good fit of all regions. After production shut-in, the model predicts an almost constantly high activity, only slowly decaying due to the stress release by the earthquakes. Therefore, the model was not able to correctly forecast the observed decrease in seismicity in the region around Eleveld after 2005, when the reservoir pressure reduction almost fully stopped. In addition, the model not only neglects aftershocks but predicts a decreased activity level after an earthquake.

Based on the work of Segall & Fitzgerald (1998) and Zoback (2010), the model of Dempsey & Suckale (2017) assumes poroelastic contraction as earthquake generation mechanism. An earthquake nucleates if a critical stress level is exceeded over a critical slip distance resulting in a slip-weakening instability (Uenishi & Rice, 2003). A fractal model determines the initial stress profile on the one-dimensional faults. The rupture propagation on those heterogeneous faults is calculated by solving the equation of motion for two tips of an expanding crack (Eshelby, 1969; Dempsey & Suckale, 2016). However, to reduce computational costs, the fault system was restricted to the 325 largest faults represented as 1-D line segments. An ensemble approach was chosen to account for unknown initial conditions by selecting a different realisation of the initial shear stress profile for each simulation. In contrast to the other hybrid models, the earthquake magnitudes are directly determined by the model. Based on the best model describing the seismicity from 1991 to 2017, forecasts of seismicity rates and magnitudes were obtained for the period 2017 to 2024 according to three production scenarios. The key parameters were determined by a Bayesian approach. The model forecasts a rapid drop in seismicity rates after production reduction and results in a widely varying range of felt earthquakes with almost the same expected maximum magnitude for the three production scenarios.

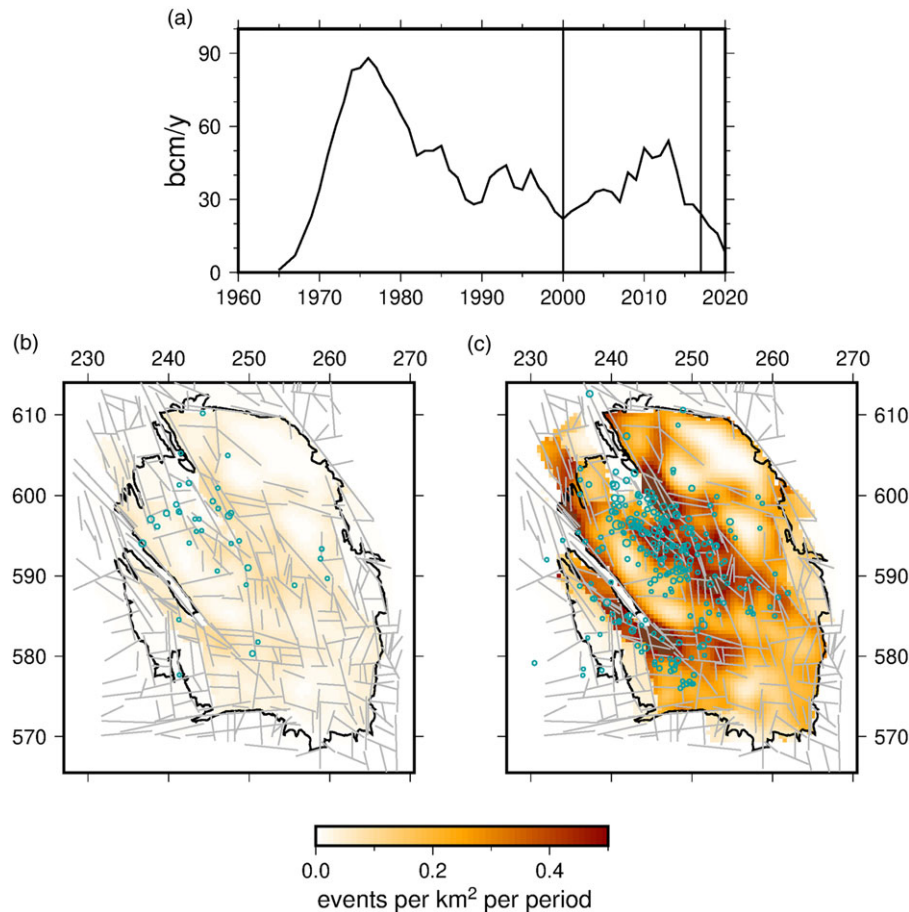


Fig. 2. (a) Overview of the gas production from the Groningen field from 1960 to 2020 adapted from NAM (2016) and gas production data from NAM (2022). The unit is billion cubic metre per year (Bcm/y). Vertical lines delimit the times of the seismicity snapshots shown at the bottom. (b) and (c) Seismicity modelled using the rate-state Coulomb model described in Richter et al. (2020) compared to observed seismicity $M \geq 1.5$ for the time periods (b) 1960–2000 and (c) 2000–2017. The model fitting period is 1960–2017. The thick black line comprises the region of the Groningen gas field and grey lines indicate the largest faults as given by Dempsey & Suckale (2017). The regions of amplified seismicity rates correspond to higher fault densities.

Advantageously, the model combines a deterministic description of the earthquake nucleation and rupture propagation with a probabilistic determination of uncertain parameters and the seismic catalogue. However, it suffers from limitations: the sensitivity to the selection of the faults and their orientations was not investigated, only the total field seismicity rate was modelled without any spatial resolution, and earthquake–earthquake interactions were not considered.

Candela et al. (2019) employed a semi-analytic approach to calculate the Coulomb stress on faults dividing the reservoir into compartments resulting in differential compaction. The approach takes into account 3-D faults, especially the vertical offset of the faults (Van Wees et al., 2019), and the pressure history combined with the Dieterich (1994) RS model to obtain the spatiotemporal distribution of seismicity rates. The poroelastic change in CFS along the faults was computed on a metre scale, but finally, only the maximum Coulomb stressing rate was used for each vertical section. Candela et al. (2019) successfully modelled the first-order spatiotemporal distribution of observed seismicity for two sub-areas of the Groningen gas field, the region exhibiting the highest seismic activity within the central area and a second area to the south-west. For some years, the number of observed earthquakes lay outside the 95% confidence interval of the model rates, which may be caused by aftershocks, short-period stress perturbations, or uncertainties in the stress or seismicity model. The analysis explained the observed differences in the seismicity response between the two sub-areas by different fault frictional responses. A subsequent study confirmed that spatial heterogeneity in the fault frictional response is required even after honouring the spatial

heterogeneity in stress development across the Groningen gas field (Candela et al., 2022). However, Candela et al. (2019, 2022) employed the seismicity rate in 1993 as apparent background rate, which constitutes a critical assumption since it disregards the most intensive production period (Fig. 2a). Thus, a large part of the most probably spatially heterogeneous pre-stressing history is not included. In addition, the model does not account for event magnitudes.

Heimisson et al. (2022) tested a revised RS model called the threshold RS (TRS) model, which takes into account that seismic sources can initially be far from instability. They applied the TRS model to the Groningen field using the maximum Coulomb stress estimated by Smith et al. (2021) 5 m above the top of the reservoir. The RS and TRS models result in comparable spatial distributions of earthquakes in good agreement with the observations, but the TRS model's fit to the observed time-varying seismicity rate is superior, better reproducing its onset, peak and decline.

Richter et al. (2020) tested the RS model of Dieterich (1994) for the Groningen field employing a simplified set-up. Instead of detailed CFS calculations, they assumed a simple proportionality of CFS to pore pressure changes and compaction strain and compared the results of the RS model with those of the Coulomb failure model. In particular, the RS formula was solved by describing the stress history as a succession of steps (Hainzl et al., 2010), and the stress field was based on the annual pore pressure and compaction data from a 2-D model provided by NAM. The fault distribution as defined by Dempsey & Suckale (2017) was taken into account as fault density map, implemented as a factor varying the background seismicity rate. The inclusion of

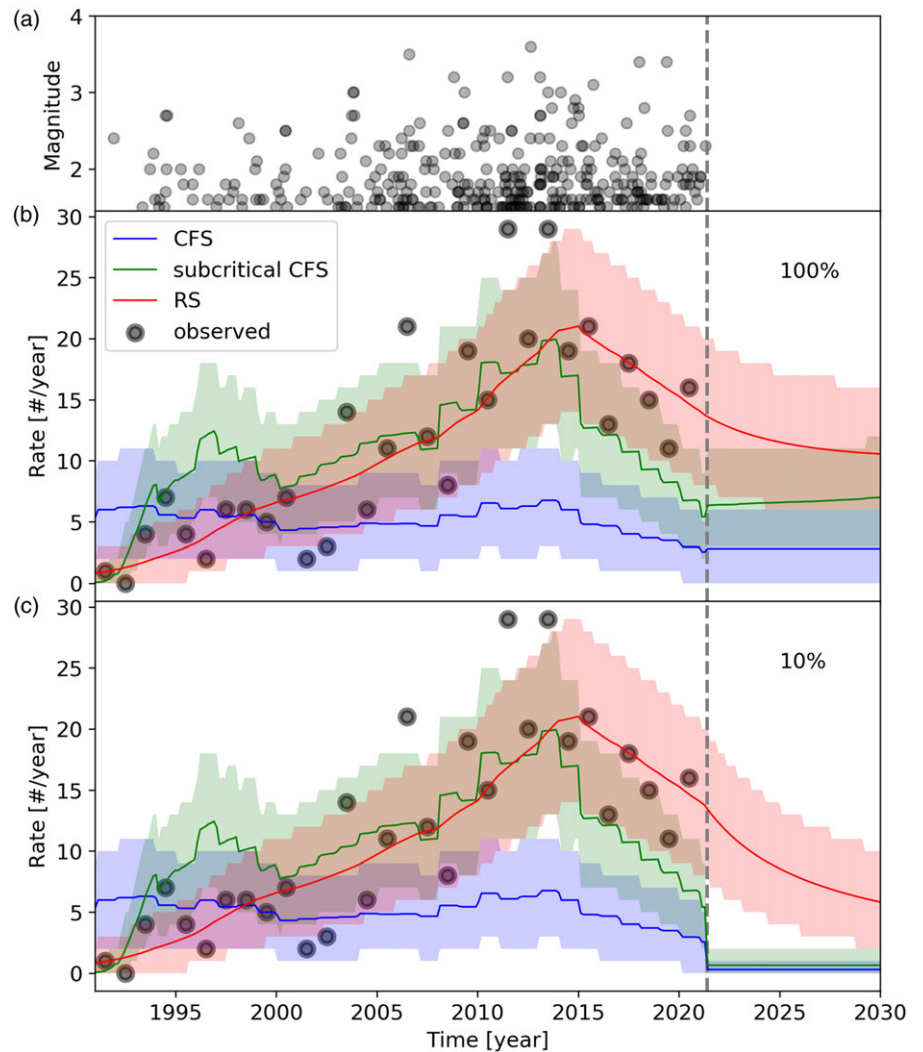


Fig. 3. Application of the Coulomb (CFS), subcritical Coulomb (CFSSub) and rate-state (RS) Coulomb model to the Groningen data. (a) Observed earthquake sequence of $M \geq 1.5$ events. (b) and (c) Comparison of modelled (lines) and observed (dots) rates. Shaded areas correspond to 90% confidence intervals according to the Poisson model. The vertical dashed line denotes the end of the fitting period, and extensions to the right are based on two different scenarios: the stressing rate in the future is (b) 100% or (c) 10% of the last year's value.

the fault density improved the models significantly and explained prominent spatial patterns of the seismicity. The best-fitting model was found to be the RS model based on pore pressure (Fig. 2b and c). In particular, the sparse seismicity before the year 2000 and the subsequently increasing number of events, focused on the zones of high fault density in the central part of the field, can be recognised. The seismic density is overestimated in the southern part of the field where more E–W striking faults are located and the homogeneous model assumptions are insufficient.

Figure 3 shows a fit of the models illustrated in Richter et al. (2020) updated until summer 2021. Again, the RS model provides the best fit to the observations, well explaining the acceleration and decay of the activity before and after 2015. The CFS model, assuming a proportionality between the stress and earthquake rate, cannot explain the data, potentially because the initial stress state was subcritical. Indeed, the subcritical CFS model (CFSSub), which requires that a critical stress state is reached locally to initialise earthquake nucleation, fits significantly better than the CFS model, but still worse than the RS model. The corresponding information gain (Rhoades et al., 2014) per event relative to the Poisson model is 0.26, 1.37 and 1.50 for CFS, CFSSub and RS model, respectively.

Beside the oversimplification of the stressing history, the models tested by Richter et al. (2020) provide no information on event magnitudes and ignore earthquake interactions. For

demonstration purposes, we combined the models with the ETAS approach to account for aftershock generation. To this end, we used the calculated rates $r(t)$ of the CFS, CFSSub and RS model as background activity for the ETAS model (Ogata, 1988). In particular, we considered the earthquake rate as:

$$R(t) = f \cdot r(t) + \sum_{i: t_i < t} K \cdot 10^{\alpha(m_i - 1.45)} \cdot (c + t - t_i)^{-p}, \quad (1)$$

calculated for earthquakes with magnitudes larger than 1.45. Here, c and p are parameters of the Omori–Utsu law (Utsu et al., 1995), while K and α describe aftershock productivity. The pre-factor f is needed to re-scale the background rate. Because the earthquake number is too small to constrain the fit of all five parameters, we assume typical parameter values, $K = 0.018$, $\alpha = 0.8$, $c = 0.01$ days and $p = 1.1$. The only free parameter is f , which was fitted by the maximum likelihood method. The resulting model trends accounting for aftershocks are shown in Fig. 4. The fit of the RS model has improved even more. Especially, the years with high observed seismicity rates are explained better. For two simplified production scenarios, we ran 10,000 forward simulations to calculate the expected mean rate and the confidence intervals. In the first case, production continues in the same manner, while in the second case, it is strongly reduced.

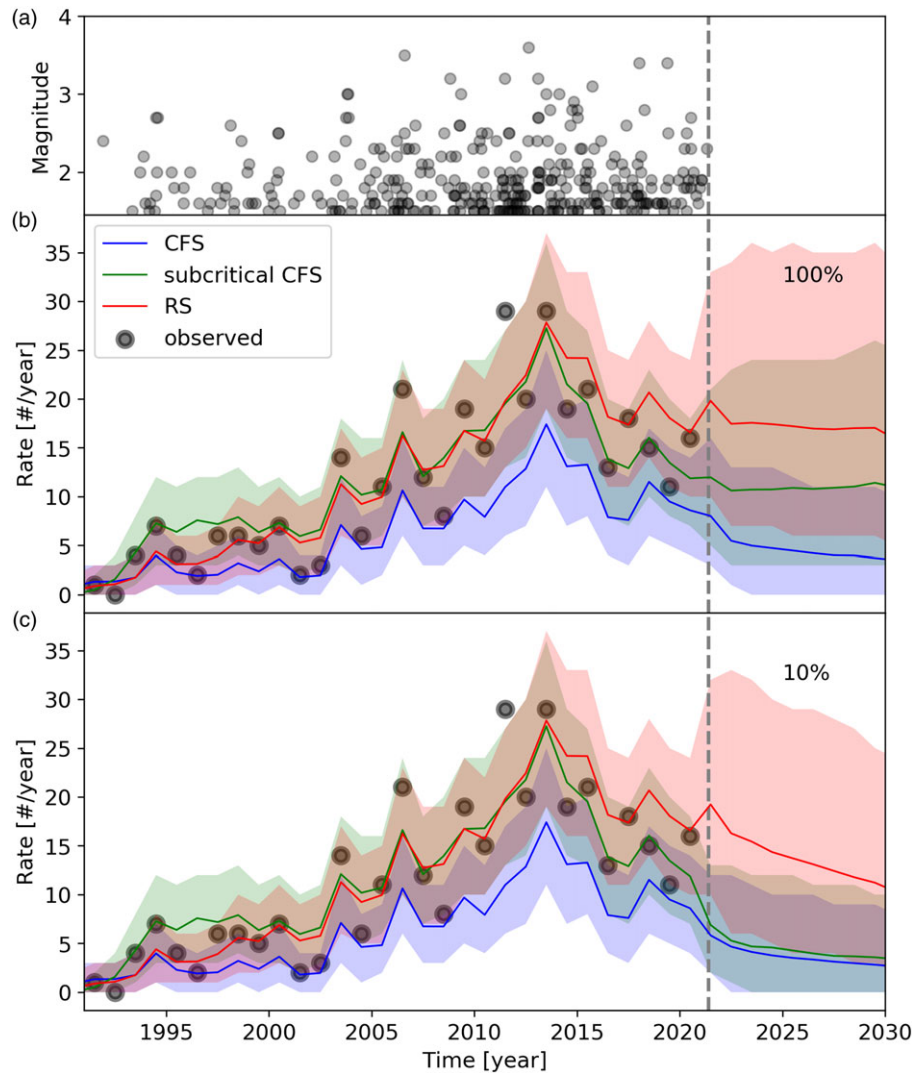


Fig. 4. Comparing the Coulomb (CFS), subcritical Coulomb (CFSsub) and rate-state (RS) Coulomb model including the ETAS approach for aftershock generation. For details, see Fig. 3.

In particular, we assume that the local stress changes per year remain the same or drop to 10% of the last period. Compared to the model forecasts disregarding aftershocks, the models combined with ETAS forecast on average higher rates and wider confidence intervals.

Probably, the most sophisticated seismogenic model for the Groningen field is the NAM hybrid model (Bourne & Oates, 2017a; Bourne et al., 2018). It was introduced by Van Elk et al. (2013) and Bourne et al. (2014) as part of a PSHA. Similar to our examples described above (Figs. 3 and 4), the NAM model predictions are based on ensembles of earthquake catalogues using Monte Carlo simulations (Bourne et al., 2014, 2015). Except for the initial version of the model, aftershock occurrence is considered employing the ETAS approach. The model underwent a considerable development from an empirical basis (Bourne et al., 2014) to a more physical and complex formulation (Bourne & Oates, 2017b; Bourne et al., 2018). A detailed review can be found in Dahm et al. (2020a). The initial version of the NAM model (Van Elk et al., 2013; Bourne et al., 2014) assumed that compaction is the main mechanism behind induced seismicity in the Groningen field and employed an empirical relation based on strain partitioning linking compaction strain and total seismic moment. A revision of the model (Bourne & Oates, 2014, 2015) changed the focus from modelling total seismic moment budget to modelling seismic

activity rate. In particular, the model was based on calculations of the time-dependent compaction strain and the assumption of statistically distributed pre-stress values, which led to a time-dependent seismicity rate modelled by an inhomogeneous Poisson model. A new framework for fault reactivation induced by poroelastic deformation (Bourne & Oates, 2017b; Bourne et al., 2018) provided an operational, stochastic- and physics-based model to account for the early spatiotemporal evolution of seismicity rates and magnitudes as a function of reservoir pore pressure, strain and lateral geometrical changes within a heterogeneous, thin-sheet reservoir. In this model, elastic and geometric reservoir heterogeneities governed the incremental Coulomb stresses induced by pore pressure changes, and under these incremental Coulomb stress loads, the weakest parts of pre-existing geological faults could experience frictional failure resulting in an induced earthquake. Structural heterogeneities are assumed to localise shear stresses and seismicity where structural gradients are greatest. These places are often associated with faults that partially offset the reservoir, and elastic heterogeneities serve to localise induced shear stresses and seismicity within the regions of greatest reservoir compressibility (Bourne & Oates, 2017b; Bourne et al., 2018). The location and geometry of faults were taken from the seismic interpretation. Faults with larger offsets were ignored because they were supposed to be aseismic due to their contact with

the overlying Zechstein salt formation. This involved the risk of excluding major faults that may become activated in the future. The elastic and geometric heterogeneities were represented by a deterministic, smoothed, poroelastic, stress–strain tensor field, which was derived using geodetic measurements of surface displacements, geophysical imaging of reservoir geometry and in-well monitoring of reservoir pore pressures (Bourne & Oates, 2017b; Bourne *et al.*, 2018). Fault friction heterogeneities localised seismicity within the weakest fault segments. Since these were located in the tail of their joint probability distribution, extreme value theory could be applied to govern the exponential-like increase in the rate of induced seismicity and an increase in expected magnitudes as the fraction of fault segments that are close to failure increases (Bourne & Oates, 2017b; Bourne *et al.*, 2018). However, once the reservoir transitions into a steady state, the seismic activity rates become proportional to induced strains leading to their overestimation. Since the parameters of frictional fault strength and initial stress heterogeneities are not directly observable, they are represented in the model by a single invariant probability distribution of initial fault stress and a transient stochastic function for stress-induced earthquake nucleation due to previous earthquakes (Bourne *et al.*, 2018). A constant observation made throughout the development of the NAM seismogenic model was the lack of sufficient data to constrain its parameters. This limitation became more accentuated as the number of model parameters increased with the model sophistication.

Recently, Smith *et al.* (2021) demonstrated that the lag and exponential onset of seismicity are well reproduced assuming either a generalised Pareto distribution of initial strength excess, as previously considered by Bourne & Oates (2017b) as well as Bourne *et al.* (2018), or a Gaussian distribution. While the former can only represent the tail of the distribution, the latter describes both its tail and body. The authors used this representation to test whether the induced seismicity at Groningen has transitioned to a steady state in which the earthquake rate is proportional to the stressing rate but found that this is not yet the case.

All of the discussed hybrid models are based partially on stress changes related to the reservoir model. Uncertainties from these as well as other input data will certainly be carried forward into the model forecasts. However, during seismic hazard computation, Monte Carlo simulations can incorporate these uncertainties in the final estimates due to the low computational costs. Different branches in the logic tree can address the epistemic uncertainties related to the reservoir model and parameter uncertainties. In contrast, aleatoric uncertainties can be quantified by a large number of stochastic forward simulations.

Discussion and concluding remarks

Open questions

The information on the 3-D reservoir and fault structures, pressure depletion, reservoir compaction, and seismicity in Groningen is comprehensive and detailed. The seismicity models for Groningen have considered most of this unique and outstanding information and are advanced. However, there are knowledge gaps in terms of process understanding as well as the role of structural and dynamic parameters controlling earthquake nucleation and rupture.

The state of stress on faults and their history is assumed to be a key factor controlling the trigger potential of earthquakes. Nevertheless, the magnitude and orientation of stress as a function of space and time is often least known, since stresses cannot be

measured directly with remote sensors and are difficult to determine *in situ*. Another crucial point in the development of more accurate fault models is the insight that salt intrusions within the faults may affect dynamic ruptures significantly, because they may introduce a rate dependency to fault movement and change the frequency-magnitude distribution of seismic events (Kettermann *et al.*, 2017). Although for Groningen, there are currently no subsurface data indicating the existence of salt-filled faults, this may only be due to technical limitations. Using analogue models, Kettermann *et al.* (2017) demonstrated that salt from the Zechstein formation might flow down-dip into opening faults due to gravitational flow.

In addition, Kortekaas & Jaarsma (2017) pointed out that the permeability structure of the Groningen reservoir is complex and highly anisotropic. Therefore, most clusters of production wells have their specific drainage areas. Another process potentially influencing pore pressure and thus Coulomb stress inside and outside the reservoir is related to the underlying aquifer system reacting to production and injections.

While much work has been done to estimate pressure and stress within the reservoir layer, the stresses outside of the field and within basement rocks have been rarely studied. Interestingly, induced seismicity in the Groningen area only occurred after a pore pressure reduction of ~10 MPa was reached (e.g., Candela *et al.*, 2018), which is often taken as evidence that before production, most regional faults were far from critical tectonic Coulomb stresses. On the other hand, North German gas fields, placed in similar Rotliegend formations and showing a similarly delayed onset of seismicity, experienced significant earthquakes on faults outside of the reservoirs (e.g., Fig. 1 in Brandes *et al.*, 2014; Dahm *et al.*, 2007; Uta, 2017). As the setting and production are comparable, and similar geomechanical fault stressing models are in use (e.g., Haug *et al.*, 2018), the seismicity models suggested for Groningen can likely be used as well to study induced seismicity in most of the North German gas fields.

A further key question concerns the partitioning of deformation between poroelastic and time-dependent inelastic components and the heterogeneity of the remaining stored elastic stress. The Groningen field contains only a single injection cluster in the east of the field. However, it is unclear whether intermediate and long-term effects from injections may impact the seismicity at larger distances. Globally, examples of causal relationships as well as far-reaching and strongly delayed effects on induced and triggered seismicity are documented (Van der Elst *et al.*, 2016; Galis *et al.*, 2017; Grigoli *et al.*, 2018).

Seismicity models for Groningen were designed to reproduce the historical seismicity for the given production and the derived Coulomb stress loading. For seismic hazard assessment, a frequency-magnitude distribution has to be assigned. Due to the limited number of recorded events, the most simple and conservative assumption is a Gutenberg–Richter distribution with a constant *b*-value combined with load-dependent productivity. However, newer models suggest implementing time- or stress-dependent variations of the distribution. For instance, Bourne & Oates (2017a) proposed the use of a stress-dependent *b*-value and Bourne & Oates (2019) the use of a stress-dependent tapered power law for larger magnitudes.

New high-precision source and rupture information combined with highly resolved fault models provide additional physical constraints that are not yet fully explored. The association of earthquake hypocentres with faults and the observed variability of seismic source mechanisms and isotropic compaction components

has not yet been considered in seismicity models developed for Groningen. For example, Kortekaas & Jaarsma (2017) derived high-resolution faults from 3-D seismic data, which seem to better correlate with recent earthquake hypocentres than previously mapped faults. Intersecting faults, as close to the 2018 Zeerijp event (Wentinck, 2018b), may accumulate stress. Therefore, such fault complexity may be related to larger induced events (see also Candela et al., 2018). Furthermore, improved detection and location of small magnitude events within the Groningen field can help to improve seismicity statistics and characterise active weak zones prior to the occurrence of large earthquakes. Such improvements might be achieved, for example, by applying novel methodologies as the highly scalable convolutional neural network presented by Perol et al. (2018) for induced seismicity in Oklahoma, USA. In general, the low number of spatially and temporally clustered earthquakes in the Groningen field (Jagt et al., 2017; Muntendam-Bos, 2020) is an obstacle for deriving relative event locations. Another feature that may significantly help to improve seismicity models is the earthquake source mechanism as analysed for the Groningen field by Willacy et al. (2018); Willacy et al. (2019); Kühn et al. (2020) and Dost et al. (2020). For specific events, kinematic rupture models have been estimated (Wentinck, 2017; Wentinck, 2018a, b, c) or derived from apparent source spectra (Ameri et al., 2020). This rupture information is not yet considered in current seismicity models. However, estimation of the kinematic and dynamic rupture parameters of such small earthquakes remains a challenge despite the monitoring network extensions in 2015.

Objective assessment and comparison of different model types

For a specific case as the Groningen field, it is a challenge to objectively evaluate and compare models against each other, since they are developed for various aims and specific targets. Physical models and deterministic scenarios were mostly developed to investigate specific aspects of the nucleation and rupture process of induced earthquakes. They cannot be directly applied in seismic hazard studies because of limited computational power as well as unknown model parameters and initial conditions. Instead, they can help to improve the process understanding and to enhance concepts for seismicity models. However, both analytical and deterministic approaches have clear limitations considering the complex nature of reservoirs, subsurface and earthquake ruptures. ML presents a possibility to bypass the problem of incomplete and potentially biased process understanding, as it extracts relevant patterns and information directly from available multivariate datasets without requiring insight into the underlying physical mechanisms. The drawbacks of the ML approaches are the limited forecasting power due to the small number of earthquakes available for model training and that future stress evolution will likely not be covered by the historical training dataset.

Empirical statistical models also avoid physical constraints but implement – in contrast to ML – parametric relations between observable characteristics and use basic statistical models to account for aleatoric variability. Statistical models can be effective for short-term forecasts, such as predicting aftershock activity by ETAS-type models or predicting cumulative seismicity. However, a weakness similar to ML is that purely statistical models cannot provide reliable predictions for system states evolving outside the range covered during the learning period.

Hybrid models combine physics-based deterministic with statistical models. In particular, they are based on modelled stress

values in the seismogenic zone and a threshold criterion leading to a forecast of the average rate. The natural variability in magnitude and time is accounted for by the statistical Gutenberg–Richter and Poisson models. Hybrid models are preferential for time-dependent hazard assessment of induced seismicity, because they can more easily adapt to changing production scenarios. Most hybrid models are based on reservoir models and reasonable physical considerations, but the validity of those assumptions is not always proven. For example, it is still debated whether to favour the RS model assuming RS-dependent friction (Bourne & Oates, 2018; Candela et al., 2019; Richter et al., 2020; Heimisson et al., 2022) or the CFS model assuming static–kinetic friction with instantaneous earthquake nucleation (Bourne et al., 2018; Richter et al., 2020; Smith et al., 2021).

Because of the large variation of parameter sets, assumptions, input data and different forecast outputs, it is almost impossible to compare and judge the performance of the alternative approaches. Further, due to the complexity of most models and the partly specific development and adaptation to the Groningen field, it remains unclear whether or not hidden parameters were set based on the knowledge of the full dataset without explicit perception of the authors. Thus, for a quantitative comparison, an independent, systematic testing approach is essential. This task has been already recognised for a long time for natural seismicity. To tackle it, the Collaboratory for the Study of Earthquake Predictability (CSEP) was established (Jordan, 2006). Within the CSEP framework, fully prospective tests of earthquake forecasts are carried out in independent testing centres using standardised statistical tests and authoritative datasets to assess the models' predictive skills and to compare them objectively. CSEP experiments use pre-defined rules to test forecasts against observations using a number of different evaluation metrics (Jordan, 2006; Zechar et al., 2010; Jordan et al., 2011; Rhoades et al., 2011; Michael & Werner, 2018; Schorlemmer & Gerstenberger, 2007; Schorlemmer et al., 2018). In addition, these include comparative metrics to statistically determine whether one model performs better than another over an evaluation period. Similar efforts have not been made so far for induced seismicity. In principle, it would be straightforward to implement a CSEP-type testing framework to validate, compare and rank the models developed for Groningen. Whether or not such a test set-up is feasible and successful depends on at least three conditions: (1) a sufficient number of earthquakes to allow for discrimination between models, (2) the willingness of model developers to participate and provide software codes that run automatically and (3) a test centre in which independent researchers run the codes.

It should be noted that although the production within the Groningen field will be terminated in the near future as decided by the Dutch government, the modelling of the seismicity after a production stop is a challenge for seismicity models because delayed processes and mechanisms can play a crucial role. For instance, a clear seismicity decrease followed the significant production reduction in 2014, but larger earthquakes of magnitudes $M \geq 3.0$ continued to occur.

Thus, the feasibility of fully prospective tests should be evaluated carefully, since a CSEP-type testing framework may provide important indications about the predictive power of the different models. In particular, the test results may provide important information on how different models should be weighted in a logic tree approach for seismic hazard assessment in so-called ensemble models. This approach would ensure the best usage of existing seismogenic models.

Acknowledgements. The project KEM-08 'Seismogenic source models for the Groningen gas reservoir' was financed by the Dutch State Supervision of Mines (SodM). The authors would like to thank Volker Oye (NORSAR) for the quality assurance of the project. Further, the authors are grateful to NAM personnel, especially Stephen Bourne, for openly discussing and explaining their source model at great length. Finally, the authors would like to thank two anonymous reviewers for their critical input that helped to improve and clarify this manuscript.

References

- Ameri, G., Martin, C. & Oth, A.**, 2020. Ground-motion attenuation, stress drop, and directivity of induced events in the Groningen gas field by spectral inversion of borehole records. *Bulletin of the Seismological Society of America* **110**(5): 2077–2094.
- Bergen, K.J., Chen, T. & Li, Z.**, 2019. Preface to the focus section on machine learning in seismology. *Seismological Research Letters* **90**(2A): 477–480.
- Bierman, S., Paleja, R. & Jones, M.**, 2018. Statistical methodology for investigating seasonal variation in rates of earthquake occurrence in the Groningen field. Technical report, Nederlandse Aardolie Maatschappij BV. Available at <https://nam-onderzoeksrapporten.data-app.nl/reports/download/groningen/en/b0a1286f-8563-46d2-a342-d5aa279d72e0>
- Bommer, J.J., Dost, B., Edwards, B., Kruiver, P.P., Ntinalexis, M., Rodriguez-Marek, A., Stafford, P.J. & Van Elk, J.**, 2017. Developing a model for the prediction of ground motions due to earthquakes in the Groningen gas field. *Netherlands Journal of Geosciences* **96**(5): s203–s213.
- Bourne, S. & Oates, S.**, 2014. An activity rate model of induced seismicity within the Groningen field. Technical report, Nederlandse Aardolie Maatschappij BV. Available at <https://nam-onderzoeksrapporten.data-app.nl/reports/download/groningen/en/71763171-e379-4eb2-91d0-29eaf6cb205c>
- Bourne, S. & Oates, S.**, 2015. An activity rate model of induced seismicity within the Groningen field (part 1). Technical report, Nederlandse Aardolie Maatschappij BV. Available at <https://nam-onderzoeksrapporten.data-app.nl/reports/download/groningen/en/8b6f2ff1-b98e-4148-a1db-bf06881579e5>
- Bourne, S. & Oates, S.**, 2017a. Development of statistical geomechanical models for forecasting seismicity induced by gas production from the Groningen field. *Netherlands Journal of Geosciences* **96**(5): s175–s182.
- Bourne, S. & Oates, S.**, 2017b. Extreme threshold failures within a heterogeneous elastic thin sheet and the spatial-temporal development of induced seismicity within the Groningen gas field. *Journal of Geophysical Research: Solid Earth* **122**(12): 10299–10320.
- Bourne, S. & Oates, S.**, 2018. The influence of stress rates on induced seismicity rates within the Groningen gas field - seismological model. Technical report, Nederlandse Aardolie Maatschappij BV. Available at <https://nam-onderzoeksrapporten.data-app.nl/reports/download/groningen/en/e0cd632a-8e06-48bd-b65c-e3afd5110ed3>
- Bourne, S. & Oates, S.**, 2019. Evolution of induced earthquake magnitude distributions with increasing stress in the Groningen gas field. Technical report, Nederlandse Aardolie Maatschappij BV. Available at <https://nam-onderzoeksrapporten.data-app.nl/reports/download/groningen/en/7ac27ead-c59e-418b-9d1f-3897a96021d7>
- Bourne, S., Oates, S., Van Elk, J. & Doornhof, D.**, 2014. A seismological model for earthquakes induced by fluid extraction from a subsurface reservoir. *Journal of Geophysical Research: Solid Earth* **119**(12): 8991–9015.
- Bourne, S., Oates, S., Bommer, J., Dost, B., Van Elk, J. & Doornhof, D.**, 2015. A Monte Carlo method for probabilistic hazard assessment of induced seismicity due to conventional natural gas production. *Bulletin of the Seismological Society of America* **105**(3): 1721–1738.
- Bourne, S., Oates, S. & Van Elk, J.**, 2018. The exponential rise of induced seismicity with increasing stress levels in the Groningen gas field and its implications for controlling seismic risk. *Geophysical Journal International* **213**(3): 1693–1700.
- Brandes, C., Steffen, H., Bönemann, C., Plenefisch, T., Gestermann, N. & Winsemann, J.**, 2014. Aktive Tektonik in Norddeutschland: glazial-isostatische Ausgleichsbewegungen und/oder Folgen der Erdöl/Erdgas-Förderung? *Erdöl Erdgas Kohle* **130**(4): 138–143.
- Broccardo, M., Mignan, A., Wiemer, S., Stojadinovic, B. & Giardini, D.**, 2017. Hierarchical Bayesian modeling of fluid-induced seismicity. *Geophysical Research Letters* **44**(22): 11,357–11,367.
- Buijze, L., van den Bogert, P., Wassing, B., Orlic, B. & ten Veen, J.**, 2017. Fault reactivation mechanisms and dynamic rupture modelling of depletion-induced seismic events in a Rotliegend gas reservoir. *Netherlands Journal of Geosciences* **96**(5): s131–s148.
- Buijze, L., van den Bogert, P., Wassing, B. & Orlic, B.**, 2019. Nucleation and arrest of dynamic rupture induced by reservoir depletion. *Journal of Geophysical Research: Solid Earth* **124**(4): 3620–3645.
- Candela, T., Wassing, B., Ter Heege, J. & Buijze, L.**, 2018. How earthquakes are induced. *Science* **360**(6389): 598–600.
- Candela, T., Osinga, S., Ampuero, J.-P., Wassing, B., Pluymaekers, M., Fokker, P., van Wees, J.-D., de Waal, H. & Muntendam-Bos, A.**, 2019. Depletion-induced seismicity at the Groningen gas field: Coulomb rate-and-state models including differential compaction effect. *Journal of Geophysical Research: Solid Earth* **124**(7): 7081–7104.
- Candela, T., Pluymaekers, M., Ampuero, J.-P., van Wees, J.-D., Buijze, L., Wassing, B., Osinga, S., Grobde, N. & Muntendam-Bos, A.**, 2022. Controls on the spatio-temporal patterns of induced seismicity in Groningen constrained by physics-based modelling with Ensemble-Smoother data assimilation. *Geophysical Journal International* **229**(2): 1282–1308.
- Dahm, T., Krüger, F., Stammer, K., Klinge, K., Kind, R., Wylegalla, K. & Grasso, J.R.**, 2007. The 2004 M_w 4.4 Rotenburg, Northern Germany, earthquake and its possible relationship with gas recovery. *Bulletin of the Seismological Society of America* **97**(3): 691–704.
- Dahm, T., Hainzl, S., Kühn, D., Oye, V., Richter, G. & Vera Rodriguez, I.**, 2020a. Review of seismogenic source models for the Groningen gas reservoir, WP1: review of the existing NAM seismogenic source model. Technical report, NORSAR. Available at https://www.norsar.no/getfile.php/1312707-1634823402/norsar.no/R-D/SodM_seismicity_source_model_review_WP1_final-signed.pdf
- Dahm, T., Hainzl, S., Kühn, D., Oye, V., Richter, G. & Vera Rodriguez, I.**, 2020b. Review of seismogenic source models for the Groningen gas reservoir, WP2: review of existing alternative approaches and possible knowledge gaps. Technical report, NORSAR. Available at https://www.norsar.no/getfile.php/1312710-1634823405/norsar.no/R-D/SodM_seismicity_source_model_review_WP2_final-signed.pdf
- DeDontney, N.**, 2017. Groningen seismological models for activity rate forecasting. Technical report, Nederlandse Aardolie Maatschappij BV. Available at <https://nam-onderzoeksrapporten.data-app.nl/reports/download/groningen/en/bafb15b2-2d77-4b80-8a5f-3f6ffc605795>
- DeDontney, N. & Lele, S.**, 2018. Impact of production fluctuations on Groningen seismicity – geomechanical modelling using rate and state friction. Technical report, Nederlandse Aardolie Maatschappij BV. Available at <https://nam-onderzoeksrapporten.data-app.nl/reports/download/groningen/en/6b2e9b94-a995-4089-864a-67ec5fda839>
- De Jager, J. & Visser, C.**, 2017. Geology of the Groningen field-an overview. *Netherlands Journal of Geosciences* **96**(5): s3–s15.
- Dempsey, D. & Suckale, J.**, 2016. Collective properties of injection-induced earthquakes sequences: 1. Model description and directivity bias. *Journal of Geophysical Research: Solid Earth* **121**: 3609–3637.
- Dempsey, D. & Suckale, J.**, 2017. Physics-based forecasting of induced seismicity at Groningen gas field, the Netherlands. *Geophysical Research Letters* **44**(15): 7773–7782.
- Dieterich, J.**, 1994. A constitutive law for rate of earthquake production and its application to earthquake clustering. *Journal of Geophysical Research: Solid Earth* **99**(B2): 2601–2618.
- Dost, B., Ruigrok, E. & Spetzler, J.**, 2017. Development of seismicity and probabilistic hazard assessment for the Groningen gas field. *Netherlands Journal of Geosciences* **96**(5): s235–s245.
- Dost, B., van Stiphout, A., Kühn, D., Kortekaas, M., Ruigrok, E. & Heimann, S.**, 2020. Probabilistic moment tensor inversion for hydrocarbon-induced seismicity in the Groningen gas field, the Netherlands, part 2: application. *Bulletin of the Seismological Society of America* **110**(5): 2112–2123.

- Eshelby, J.**, 1969. The elastic field of a crack extending non-uniformly under general anti-plane loading. *Journal of the Mechanics and Physics of Solids* 17(3): 177–199.
- Galis, M., Ampuero, J.P., Mai, P.M. & Cappa, F.**, 2017. Induced seismicity provides insight into why earthquake ruptures stop. *Science Advances* 3(12): eaap7528.
- Geertsma, J.**, 1973. A basic theory of subsidence due to reservoir compaction: the homogeneous case. *Verhandelingen Koninklijk Nederlands Geologisch Mijnbouwkundig Genootschap* 28: 43–62.
- Grigoli, F., Cesca, S., Rinaldi, A.P., Manconi, A., Lopez-Comino, J.A., Clinton, J.F., Westaway, R., Cauzzi, C., Dahm, T., Wiemer, S.**, 2018. The November 2017 Mw 5.5 Pohang earthquake: a possible case of induced seismicity in South Korea. *Science* 360(6392): 1003–1006.
- Hainzl, S., Steacy, S. & Marsan, D.**, 2010. Seismicity models based on Coulomb stress calculations, Community Online Resource for Statistical Seismicity Analysis. Available at http://www.corrssa.org/export/sites/corrssa/galleries/articles-pdf/Hainzl-et-al-2010-CORSSA-Coulomb-models.pdf_2063069299.pdf
- Hastie, T., Tibshirani, R. & Friedman, J.**, 2009. *The elements of statistical learning*. Springer (New York).
- Haug, C., Nüchtern, J.-A. & Henk, A.**, 2018. Assessment of geological factors potentially affecting production-induced seismicity in North German gas fields. *Geomechanics for Energy and the Environment* 16: 15–31.
- Heimisson, E.R., Smith, J.D., Avouac, J.P. & Bourne, S.J.**, 2022. Coulomb threshold rate-and-state model for fault reactivation: application to induced seismicity at Groningen. *Geophysical Journal International* 228(3): 2061–2072.
- Hettema, M.H.H., Jaarsma, B., Schroot, B.M. & van Yperen, G.C.N.**, 2017. An empirical relationship for the seismic activity rate of the Groningen gas field. *Netherlands Journal of Geosciences* 96(5): s149–s161.
- Hofman, L.J., Ruigrok, E., Dost, B. & Paulssen, H.**, 2017. A shallow seismic velocity model for the Groningen area in the Netherlands. *Journal of Geophysical Research Solid Earth* 122(10): 8035–8050.
- Jagt, L., Ruigrok, E. & Paulssen, H.**, 2017. Relocation of clustered earthquakes in the Groningen gas field. *Netherlands Journal of Geosciences* 96(5): s163–s173.
- Jansen, J., Singhal, P. & Vossepoel, F.**, 2019. Insights from closed-form expressions for injection-and production-induced stresses in displaced faults. *Journal of Geophysical Research: Solid Earth* 124(7): 7193–7212.
- Jordan, T.H.**, 2006. Earthquake predictability, brick by brick. *Seismological Research Letters* 77(1): 3–6.
- Jordan, M.I. & Mitchell, T.M.**, 2015. Machine learning: trends, perspectives, and prospects. *Science* 349(6245): 255–260.
- Jordan, T.H., Chen, Y.-T., Gasparini, P., Madariaga, R., Main, I., Marzocchi, W., Papadopoulos, G., Sobolev, G., Yamaoka, K., Zschau, J.**, 2011. Operational earthquake forecasting. State of knowledge and guidelines for utilization. *Annals of Geophysics* 54(4). doi: 10.4401/ag-5350.
- Kettermann, M., Abe, S., Raith, A.F., de Jager, J. & Urai, J.L.**, 2017. The effect of salt in dilatant faults on rates and magnitudes of induced seismicity – first results building on the geological setting of the Groningen Rotliegend reservoirs. *Netherlands Journal of Geosciences* 96(5): s87–s104.
- King, G.C.P., Stein, R.S. & Lin, J.**, 1994. Static stress changes and the triggering of earthquakes. *Bulletin of the Seismological Society of America* 84(3): 935–953.
- Kortekaas, M. & Jaarsma, B.**, 2017. Improved definition of faults in the Groningen field using seismic attributes. *Netherlands Journal of Geosciences* 96(5): s71–s85.
- Kruiver, P.P., Van Dedem, E., Romijn, R., de Lange, G., Korff, M., Stafleu, J., Gunnink, J.L., Rodriguez-Marek, A., Bommer, J.J., Van Elk, J., Doornhof, D.**, 2017. An integrated shear-wave velocity model for the Groningen gas field, The Netherlands. *Bulletin of Earthquake Engineering* 15(9): 3555–3580.
- Kühn, D., Heimann, S., Isken, M.P., Ruigrok, E. & Dost, B.**, 2020. Probabilistic moment tensor inversion for hydrocarbon-induced seismicity in the Groningen gas field, the Netherlands, part 1: testing. *Bulletin of the Seismological Society of America* 110(5): 2095–2111.
- Langenbruch, C. & Zoback, M.D.**, 2016. How will induced seismicity in Oklahoma respond to decreased saltwater injection rates? *Science Advances* 2(11): e1601542.
- Lanz, F., Bisdom, K., Barbaro, E., Limbeck, J., Park, T., Harris, C. & Nevenzeel, K.**, 2019. Evaluation of a machine learning methodology for spatio-temporal induced seismicity forecasts within the Groningen field - machine learning. Technical report, Nederlandse Aardolie Maatschappij BV. Available at <https://nam-onderzoeksrapporten.data-app.nl/reports/download/groningen/en/e5535713-46e2-4523-a479-4124f674c55f>
- Lele, S.P., Hsu, S.-Y., Garzon, J.L., DeDontney, N., Searles, K.H., Gist, G.A. & Dale, B.A.**, 2016. Geomechanical modeling to evaluate production-induced seismicity at Groningen gas field. Abu Dhabi International Petroleum Exhibition and Conference. Society of Petroleum Engineers (Abu Dhabi).
- Limbeck, J., Lanz, F., Barbaro, E., Harris, C., Bisdom, K., Park, T., Oosterbosch, W., Jamali-Rad, H. & Nevenzeel, K.**, 2018. Evaluation of a machine learning methodology to forecast induced seismicity event rates within the Groningen field. Technical report, Nederlandse Aardolie Maatschappij BV. Available at <https://nam-onderzoeksrapporten.data-app.nl/reports/download/groningen/en/d5be89f6-fcea-4237-bc07-6cda25e151d9>
- Michael, A.J. & Werner, M.J.**, 2018. Preface to the focus section on the Collaboratory for the Study of Earthquake Predictability (CSEP): new results and future directions. *Seismological Research Letters* 89(4): 1226–1228.
- Muntendam-Bos, A.**, 2020. Clustering characteristics of gas-extraction induced seismicity in the Groningen gas field. *Geophysical Journal International* 221(2): 879–892.
- NAM**, 2016. Winningsplan Groningen Gasveld 2016. Technical report, Nederlandse Aardolie Maatschappij BV. Available at <https://nam-onderzoeksrapporten.data-app.nl/reports/download/groningen/nl/c7f20ac1-1818-4f2f-82b0-b347fa2455aa>
- NAM**, 2022. Gas- en olie productiecijfers. Available at https://www.nam.nl/gas-en-olie/gaswinning.html#iframe=L2VtYmVkL2NvbXBvbmVudC8_aWQ9Z2Zd2lubmluZwD, last accessed on 03 March 2022.
- Nepveu, M., van Thienen-Visser, K. & Sijacic, D.**, 2016. Statistics of seismic events at the Groningen field. *Bulletin of Earthquake Engineering* 14(12): 3343–3362.
- Ogata, Y.**, 1988. Statistical models for earthquake occurrence and residual analysis for point processes. *Journal of the American Statistical Association* 83(401): 9–27.
- Ogata, Y.**, 1998. Space-time point-process models for earthquake occurrences. *Annals of the Institute of Statistical Mathematics* 50(2): 379–402.
- Okada, Y.**, 1992. Internal deformation due to shear and tensile faults in a half-space. *Bulletin of the Seismological Society of America* 82(2): 1018–1040.
- Park, T. & Nevenzeel, K.**, 2018. A simulation study into the detectability threshold for seasonal variations in earthquake occurrence rates within the Groningen field - Machine Learning. Technical report, Nederlandse Aardolie Maatschappij BV. Available at <https://nam-onderzoeksrapporten.data-app.nl/reports/download/groningen/en/314e2dd3-96a3-42b7-ba6c-213d66e7c143>
- Park, T., Jamali-Rad, H., Oosterbosch, W., Limbeck, J., Lanz, F., Harris, C., Barbaro, E., Bisdom, K. & Nevenzeel, K.**, 2018. Seasonality analysis for induced seismicity event rate time series within the Groningen field - Machine Learning. Technical report, Nederlandse Aardolie Maatschappij BV. Available at <https://nam-onderzoeksrapporten.data-app.nl/reports/download/groningen/en/6bce70a2-3c0a-4698-a03a-a79c6efa6f02>
- Perol, T., Gharbi, M. & Denolle, M.**, 2018. Convolutional neural network for earthquake detection and location. *Science Advances* 4(2): e1700578.
- Post, R.A., Michels, M.A., Ampuero, J.P., Candela, T., Fokker, P.A., van Wees, J.D., van der Hofstad, R.W. & van den Heuvel, E.R.**, 2021. Interevent-time distribution and aftershock frequency in non-stationary induced seismicity. *Scientific Reports* 11(1): 1–10.
- Rhoades, D.A., Schorlemmer, D., Gerstenberger, M.C., Christophersen, A., Zechar, J.D. & Imoto, M.**, 2011. Efficient testing of earthquake forecasting models. *Acta Geophysica* 59(4): 728–747.
- Rhoades, D.A., Gerstenberger, M.C., Christophersen, A., Zechar, J.D., Schorlemmer, D., Werner, M.J. & Jordan, T.H.**, 2014. Regional earthquake likelihood models II: information gains of multiplicative hybrids. *Bulletin of the Seismological Society of America* 104(6): 3072–3083.
- Richter, G., Hainzl, S., Dahm, T. & Zöller, G.**, 2020. Stress-based, statistical modeling of the induced seismicity at the Groningen gas field, the Netherlands. *Environmental Earth Sciences* 79(252): 1–15.

- Ruina, A., 1983. Slip instability and state variable friction laws. *Journal of Geophysical Research: Solid Earth* **88**(B12): 10359–10370.
- Sanz, P.F., Lele, S.P., Searles, K.H., Hsu, S.-Y., Garzon, J.L., Burdette, J.A., Kline, W.E., Dale, B.A. & Hector, P.D., 2015. Geomechanical analysis to evaluate production-induced fault reactivation at Groningen gas field. SEG Annual Technical Conference and Exhibition, Houston, TX. Conference proceedings.
- Schorlemmer, D. & Gerstenberger, M.C., 2007. RELM testing center. *Seismological Research Letters* **78**(1): 30–36.
- Schorlemmer, D., Werner, M.J., Marzocchi, W., Jordan, T.H., Ogata, Y., Jackson, D.D., Mak, S., Rhoades, D.A., Gerstenberger, M.C., Hirata, N., Liukis, M., Maechling, P.J., Strader, A., Taroni, M., Wiemer, S., Zechar, J.D., Zhuang, J., 2018. The laboratory for the study of earthquake predictability: achievements and priorities. *Seismological Research Letters* **89**(4): 1305–1313.
- Segall, P., 1989. Earthquakes triggered by fluid extraction. *Geology* **17**(10): 942–946.
- Segall, P. & Fitzgerald, S., 1998. A note on induced stress changes in hydrocarbon and geothermal reservoirs. *Tectonophysics* **289**: 117–128.
- Shapiro, S., 2018. Seismogenic index of underground fluid injections and productions. *Journal of Geophysical Research: Solid Earth* **123**(9): 7983–7997.
- Shapiro, S.A., Dinske, C., Langenbruch, C. & Wenzel, F., 2010. Seismogenic index and magnitude probability of earthquakes induced during reservoir fluid stimulations. *The Leading Edge* **29**(3): 304–309.
- Smith, J.D., Heimisson, E.R., Bourne, S. & Avouac, J.P., 2021. Stress-based forecasting of induced seismicity with instantaneous earthquake failure functions: applications to the Groningen Gas Reservoir. Preprint submitted to Earth ArXiv.
- Spiers, C.J., Hangx, S.J.T. & Niemeijer, A.R., 2017. New approaches in experimental research on rock and fault behaviour in the Groningen gas field. *Netherlands Journal of Geosciences* **96**(5): s55–s69.
- Uenishi, K. & Rice, J.R., 2003. Universal nucleation length for slip-weakening rupture instability under nonuniform fault loading. *Journal of Geophysical Research: Solid Earth* **108**(B1): 2042.
- Uta, P., 2017. Recent intraplate earthquakes in Northwest Germany: glacial isostatic adjustment and/or a consequence of hydrocarbon production? PhD Thesis. Gottfried Wilhelm Leibniz Universität Hannover (Hannover).
- Utsu, T., Ogata, Y. & Matsu'ura, R.S., 1995. The centenary of the Omori formula for a decay law of aftershock activity. *Journal of Physics of the Earth* **43**(1): 1–33.
- Van den Bogert, P.A.J., 2018. Depletion-induced fault slip and seismic rupture - 2D geomechanical models for the Groningen field, the Netherlands. Technical report, Nederlandse Aardolie Maatschappij BV. Available at <https://nam-onderzoeksrapporten.data-app.nl/reports/download/groningen/en/d77787dc-4e7d-4c1f-b6ee-ec29762c3b6>
- Van der Elst, N.J., Page, M.T., Weiser, D.A., Goebel, T.H. & Hosseini, S.M., 2016. Induced earthquake magnitudes are as large as (statistically) expected. *Journal of Geophysical Research: Solid Earth* **121**(6): 4575–4590.
- Van Eck, T., Goutbeek, F., Haak, H. & Dost, B., 2006. Seismic hazard due to small-magnitude, shallow-source, induced earthquakes in the Netherlands. *Engineering Geology* **87**(1-2): 105–121.
- Van Elk, J., Doornhof, D., Bourne, S., Oates, S., Bommer, J., Visser, C., van Eijs, R. & van den Bogert, P., 2013. Technical addendum to the winnings-plan Groningen 2013: subsidence, induced earthquakes and seismic hazard analysis in the Groningen field. Technical report, Nederlandse Aardolie Maatschappij BV. Available at <https://nam-onderzoeksrapporten.data-app.nl/reports/download/groningen/en/59c423ed-8ebc-4337-be7c-1d8134baa5bd>
- Van Oeveren, H., Valvatne, P., Geurtsen, L. & Van Elk, J., 2017. History match of the Groningen field dynamic reservoir model to subsidence data and conventional subsurface data. *Netherlands Journal of Geosciences* **96**(5): s47–s54.
- Van Thienen-Visser, K. & Fokker, P.A., 2017. The future of subsidence modelling: compaction and subsidence due to gas depletion of the Groningen gas field in the Netherlands. *Netherlands Journal of Geosciences* **96**(5): s105–s116.
- Van Wees, J., Buijze, L., van Thienen-Visser, K., Nepveu, M., Wassing, B., Orlic, B. & Fokker, P., 2014. Geomechanics response and induced seismicity during gas field depletion in the Netherlands. *Geothermics* **52**(7): 206–219.
- Van Wees, J.-D., Fokker, P., Van Thienen-Visser, K., Wassing, B., Osinga, S., Orlic, B., Ghouri, S., Buijze, L. & Plummaekers, M., 2017. Geomechanical models for induced seismicity in the Netherlands: inferences from simplified analytical, finite element and rupture model approaches. *Netherlands Journal of Geosciences* **96**(5): s183–s202.
- Van Wees, J.-D., Osinga, S., Van Thienen-Visser, K. & Fokker, P.A., 2018. Reservoir creep and induced seismicity: inferences from geomechanical modeling of gas depletion in the Groningen field. *Geophysical Journal International* **212**(3): 1487–1497.
- Van Wees, J.-D., Plummaekers, M., Osinga, S., Fokker, P., van Thienen-Visser, K., Orlic, B., Wassing, B., Hegen, D. & Candela, T., 2019. 3D mechanical analysis of complex reservoirs: a novel mesh-free approach. *Geophysical Journal International* **219**(2): 1118–1130.
- Visser, C.A. & Solano Viota, J.L., 2017. Introduction to the Groningen static reservoir model. *Netherlands Journal of Geosciences* **96**(5): s39–s46.
- Vlek, C., 2019. Rise and reduction of induced earthquakes in the Groningen gas field, 1991-2018: statistical trends, social impacts, and policy change. *Environmental Earth Sciences* **78**(3): 59.
- Wentinck, R., 2015. Induced seismicity in the Groningen field: a statistical assessment of tremors along faults in a compacting reservoir. Technical report, Nederlandse Aardolie Maatschappij BV. Available at <https://nam-onderzoeksrapporten.data-app.nl/reports/download/groningen/en/a283a0ed-39b0-409f-a5cf-5ec5dda6299f>
- Wentinck, H., 2017. Kinematic modelling of large tremors in the Groningen field using extended seismic sources: Huizinge earthquake part 1. Technical report, Nederlandse Aardolie Maatschappij BV. Available at <https://nam-onderzoeksrapporten.data-app.nl/reports/download/groningen/en/ae84304f-c259-48de-874f-00f5a76d36d9>
- Wentinck, H., 2018a. Dynamic modelling of large tremors in the Groningen field using extended seismic sources. Technical report, Nederlandse Aardolie Maatschappij BV. Available at <https://nam-onderzoeksrapporten.data-app.nl/reports/download/groningen/en/063425b3-f3e0-4c6f-9d85-c5fe6f0eca07>
- Wentinck, H., 2018b. Kinematic modelling of large tremors in the Groningen field using extended seismic sources: First results related to the Zeerijp tremor M_L M_L 3.4. Technical report, Nederlandse Aardolie Maatschappij BV. Available at <https://nam-onderzoeksrapporten.data-app.nl/reports/download/groningen/en/22ef5f44-6a30-4a07-bed2-3c042986e374>
- Wentinck, H., 2018c. Kinematic modelling of large tremors in the Groningen field using extended seismic sources: Huizinge earthquake part 2. Technical report, Nederlandse Aardolie Maatschappij BV. Available at <https://nam-onderzoeksrapporten.data-app.nl/reports/download/groningen/en/996f9a6e-9ef0-47e5-872d-fda8de45be8d>
- Willacy, C., van Dedem, E., Minisini, S., Li, J., Blokland, J.W., Das, I. & Droujinine, A., 2018. Application of full-waveform event location and moment-tensor inversion for Groningen induced seismicity. *The Leading Edge* **37**(2): 92–99.
- Willacy, C., van Dedem, E., Minisini, S., Li, J., Blokland, J.-W., Das, I. & Droujinine, A., 2019. Full-waveform event location and moment tensor inversion for induced seismicity. *Geophysics* **84**(2): KS39–KS57.
- Zbinden, D., Rinaldi, A.P., Urpi, L. & Wiemer, S., 2017. On the physics-based processes behind production-induced seismicity in natural gas fields. *Journal of Geophysical Research: Solid Earth* **122**(5): 3792–3812.
- Zechar, J.D., Gerstenberger, M.C. & Rhoades, D.A., 2010. Likelihood-based tests for evaluating space-rate-magnitude earthquake forecasts. *Bulletin of the Seismological Society of America* **100**(3): 1184–1195.
- Zoback, M., 2010. Reservoir geomechanics. Cambridge University Press (New York).
- Zöller, G. & Holschneider, M., 2016. The maximum possible and the maximum expected earthquake magnitude for production-induced earthquakes at the gas field in Groningen, the Netherlands. *Bulletin of the Seismological Society of America* **106**(6): 2917–2921.